Josephson effects in *d*-wave superconductor junctions with magnetic interlayers

Brian M. Andersen,[1,3] Yu. S. Barash,[2] S. Graser,[3] and P. J. Hirschfeld[3]
[1]*Nano-Science Center, Niels Bohr Institute, University of Copenhagen, Universitetsparken 5, DK-2100 Copenhagen, Denmark*
[2]*Institute of Solid State Physics, Russian Academy of Sciences, Chernogolovka, Moscow Region 142432, Russia*
[3]*Department of Physics, University of Florida, Gainesville, Florida 32611-8440, USA*
(Received 10 October 2007; published 4 February 2008)

We calculate the dc supercurrent through a Josephson tunnel junction consisting of an antiferromagnetic or ferromagnetic interlayer sandwiched between two *d*-wave superconductors (*d*). Such junctions exhibit a rich dependence of the Josephson current on the interlayer parameters, including the possibility of 0-π transitions with varying temperature or interlayer thickness. Furthermore, we study $d/I/d$ junctions when the *d*-wave superconductor leads include subdominant magnetic correlations. Induced magnetism near the interface can strongly diminish the critical current for 110 oriented junctions whereas no suppression exists for the 100 orientation. This may help resolve a long-standing puzzle of the critical current versus grain boundary angle in high-T_c superconductors.

DOI: 10.1103/PhysRevB.77.054501 PACS number(s): 74.45.+c, 74.50.+r, 74.72.−h, 75.50.Ee

I. INTRODUCTION

Interfaces and Josephson junctions between superconductors and magnetic materials can generate low-energy spin-dependent Andreev bound states leading to highly unconventional quantum transport properties. For instance, junctions consisting of *s*-wave superconductors (*s*) and ferromagnetic (F) metals have attracted great interest in recent years.[1] Such junctions have been shown to exhibit so-called 0-π transitions,[2,3] where, depending on the temperature T and the width L of the interlayer, the ground state is characterized by an internal phase difference of π between the two superconductors. This effective negative Josephson coupling is similar to what can happen when tunneling through magnetic impurities.[4] The possibility of 0-π transitions may be utilized as a basis for future quantum qubits,[5] constituting an important example in the field of superconducting spintronics.[6]

Another promising situation involves interfaces between antiferromagnets and superconductors. In this case, spin-dependent quasiparticle reflection at the antiferromagnetic (AF) surface, the so-called Q reflection, combined with Andreev reflection on the superconducting side, can lead to low-energy bound states with important consequences for the associated proximity effect.[7,8] Furthermore, in $s/\mathrm{AF}/s$ Josephson junctions, these bound states can enhance the critical current J_c at low T (Ref. 7) and lead to 0- or π-junction behavior depending on T and thickness of the AF interlayer.[9] For $s/\mathrm{AF}/s$ junctions, the 0-π behavior is a true even-odd effect arising from qualitatively different spectra of the Andreev bound states caused by different symmetries of the odd and even AF interfaces.[9]

Here, we study the Josephson current through in-plane $d/\mathrm{AF}/d$ tunnel junctions. Such junctions have not been studied before theoretically. Interestingly, our results are also relevant for $d/\mathrm{F}/d$ junctions. Based on both analytical calculations and numerical solutions of the Bogoliubov-de Gennes (BdG) equations, we determine the criteria for 0-π-junction behavior and predict unusual T dependence of the critical current $J_c(T)$.

Intrinsic $d/\mathrm{AF}/d$ junctions may already be present in the case of high-T_c grain boundaries (GBs) which induce AF surface states. Below, we also study the critical current through GBs by modeling them as $d/I/d$ junctions, where I is an insulating layer but where the leads contain subdominant magnetic correlations which become important near order parameter-suppressing interfaces. Both kinds of junctions mentioned above are cousins of the unconventional $d/I/d$ junctions with uncorrelated leads which exhibit an unusual $1/T$ behavior of $J_c(T)$ at low T as well as possible (depends on misorientation angle) T-induced 0-π transitions.[10,11] The experimental observation of these effects is notoriously difficult due to the complexity of the barrier interface, characterized, in particular, by facetting, twins and especially by many high transmission channels. Only recently have the main features associated with midgap state contribution to the Josephson current been observed in experiments.[12–14]

II. MODEL

The Hamiltonian is defined on a two-dimensional square lattice (lattice constant $a=1$),

$$\hat{H} = -t\sum_{\langle ij\rangle\sigma}\hat{c}^{\dagger}_{i\sigma}\hat{c}_{j\sigma} + \sum_{\langle ij\rangle}(\Delta_{ij}\hat{c}^{\dagger}_{i\uparrow}\hat{c}^{\dagger}_{j\downarrow} + \mathrm{H.c.}) - \sum_{i\sigma}\mu\hat{n}_{i\sigma} + \sum_{i} m_i(\hat{n}_{i\uparrow} - \hat{n}_{i\downarrow}). \quad (1)$$

Here, $\hat{c}^{\dagger}_{i\sigma}$ creates an electron of spin σ on the site i, t is the hopping matrix element, μ is the chemical potential, and Δ_{ij} and m_i denote the superconducting and magnetic order parameters, respectively. The associated BdG equations are given by

$$\sum_{j}\begin{pmatrix}\mathcal{K}^{+}_{ij,\sigma} & \mathcal{D}_{ij,\sigma}\\ \mathcal{D}^{*}_{ij,\sigma} & -\mathcal{K}^{-}_{ij,\sigma}\end{pmatrix}\begin{pmatrix}u_{n\sigma}(j)\\ v_{n\bar{\sigma}}(j)\end{pmatrix} = E_{n\sigma}\begin{pmatrix}u_{n\sigma}(i)\\ v_{n\bar{\sigma}}(i)\end{pmatrix}, \quad (2)$$

where $\mathcal{K}^{\pm}_{ij} = -t\delta_{\langle ij\rangle} + (\pm\sigma m_i - \mu)\delta_{ij}$, with $\sigma = +1/-1$ for up/down spin, and δ_{ij} and $\delta_{\langle ij\rangle}$ are the Kronecker delta symbols connecting on-site and nearest neighbor sites, respectively.

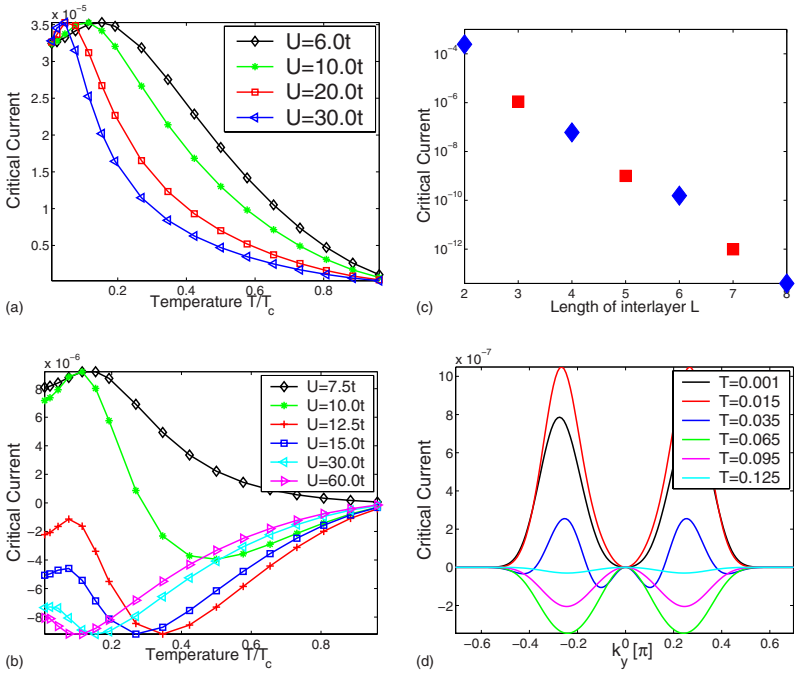

FIG. 1. (Color online) $J_c(T)$ versus T for a range of U for (a) $L=6$ and (b) $L=5$. For clarity, the curves have been normalized to give the same absolute value at the maximum as the curve with the smallest U. (c) J_c at $T=0$ as a function of interlayer thickness L. The red squares correspond to negative J_c and have been multiplied by -1 in this semilogarithmic plot. (d) The k_y-resolved current shown for $L=5$ and $U=10t$ [along green curve in (b)]. For all results shown here: $\mu=0$ and $V=t$. The latter leads to $\xi/L \sim 1$-2 in agreement with the short in-plane coherence length of cuprate superconductors.

The net magnetization is $M_i=m_i/U=\frac{1}{2}[\langle\hat{n}_{i\uparrow}\rangle-\langle\hat{n}_{i\downarrow}\rangle]$, and the off-diagonal block $\mathcal{D}_{ij}$ describes d-wave pairing $\mathcal{D}_{ij}=-\Delta_{ij}^d\delta_{\langle ij\rangle}$, where $\Delta_{ij}^d=-V\langle\hat{c}_{i\uparrow}\hat{c}_{j\downarrow}-\hat{c}_{i\downarrow}\hat{c}_{j\uparrow}\rangle/2$. The coupling constants U (V) are taken to be uniform within the antiferromagnetic (superconducting) phases, although the order parameters are allowed to vary in space though the self-consistency condition, including the proximity effect. In particular, for the junction geometry studied below, U (V) are nonzero only inside (outside) the L atomic chains constituting the AF interlayer. By Fourier transform parallel to the interface, we obtain an effective one-dimensional problem at the expense of introducing an additional parameter k_y. The dc Josephson current $j_{rr'}$ between two neighboring sites r and r' is obtained from $j_{rr'}=-(iet/\hbar)\Sigma_\sigma[\langle\hat{c}_{r\sigma}^\dagger\hat{c}_{r'\sigma}\rangle-\langle\hat{c}_{r'\sigma}^\dagger\hat{c}_{r\sigma}\rangle]$. For more details on the numerical and analytical approaches, we refer the reader to Refs. 7–9.

III. RESULTS

For $s/\mathrm{AF}/s$ junctions, the 0-π behavior as a function of interlayer thickness L exists both for 100 and 110 orientations.[9] This is not the case for $d/\mathrm{AF}/d$ junctions, where the 100 case displays only 0-junction characteristics with an Ambegaokar-Baratoff-like dependence of $J_c(T)$. Therefore, we focus on the more interesting 110 oriented $d/\mathrm{AF}/d$ junctions. We discuss only identical (and identically oriented) junctions and restrict ourselves to the tunneling limit where the current-phase relation is sinusoidal, and $J_c=J(\pi/2)$. The 110 oriented $d/\mathrm{AF}/d$ junctions are categorized further into $d/\mathrm{AF}_{\mathrm{even}}/d$ and $d/\mathrm{AF}_{\mathrm{odd}}/d$ junctions, depending on whether the interlayer consists of an even or odd number of chains with nonzero coupling U, respectively. Note that we utilize the repulsion U (or similarly m_i) to categorize the junctions, not the magnetization M_i, since it has a small component leaking into the superconducting leads by the proximity effect. Below, the thickness of the junction L is given in terms of the number of interlayer chains, and the total length of the junction is therefore $\sqrt{2}aL$. In Figs. 1(a) and 1(b), we show typical self-consistent results for J_c as a function of T for even and odd interlayer chains, respectively. As seen from Fig. 1(a), $d/\mathrm{AF}_{\mathrm{even}}/d$ are 0 junctions with a $1/T$-like dependence of J_c in the large-U limit. The small dip in J_c at low T is caused by the finite width of the interlayer and disappears in the limits $\xi/L, U\to\infty$. As shown in Fig. 1(b), $J_c(T)$ in 110 $d/\mathrm{AF}_{\mathrm{odd}}/d$ junctions exhibits a surprisingly rich T dependence: as U is increased, the pure 0 junction at low U becomes a π junction at high T, crossing over to 0-junction behavior at some T^* which eventually vanishes in the large-U limit where $J_c(T)\sim -1/T$. The systematic 0-π-junction oscillations versus interlayer thickness L is shown in Fig. 1(c). The k_y-resolved current corresponding to parameters similar to the green curve in Fig. 1(b) is shown in Fig. 1(d). The same momentum region contributes to the current at all T, a fact which will ease the analytical interpretation presented in the next section. Results qualitatively similar to those shown in Fig. 1 can also be obtained for thicker junctions with smaller values of U/t.

We now study $d/\mathrm{AF}/d$ junctions within a quasiclassical approach where, as usual, all characteristic energies are assumed to be much less than the Fermi energy E_F. We assume for the coherence length $\xi \gg a, L$, and the junction properties are conveniently expressed in terms of the scattering $\mathcal{S}$ matrix containing the reflection and transmission amplitudes. The Josephson current is carried entirely by phase-dependent Andreev bound states.

For the 100 orientation, the d-wave order parameter does not change its sign in specular reflection, but it changes sign in Q-reflection processes. Q reflection was introduced in Ref. 7 and discussed extensively in Refs. 8 and 9. In a Q-reflection event between a normal metal and an antiferro-

magnet, the momentum component of the normal quasiparticles parallel to the junction interface is changed by the y component of the AF ordering vector $\mathbf{Q}$ when y is the direction parallel to the interface. As a consequence of the nesting condition for itinerant AF phases, this leads to a reversal of the quasiparticle velocity in a Q-reflection event. Therefore, quasiparticles experience spin-dependent retro reflection at normal metal-AF transparent interfaces. In the superconducting state, the low-energy states and the Josephson transport are obtained from combined effects of Q reflection and Andreev reflection.[7–9]

In contrast to the 100 orientation, in the 110 case, the d-wave order parameter changes its sign both in specular and in Q-reflection events. An important manifestation of this physical difference between effects of Q reflection for different AF-interface orientations is that the 0-π transition does not take place for 100 orientation in d-wave junctions, but the transition is, in general, present in 110 d wave, as well as 100 s-wave junctions. More formally, in the 110 case, the specular and Q reflection possess identical outgoing group velocities and form the outgoing flow along one and the same direction. This permits the reduction of the problem to a standard situation with conventional number of incoming and outgoing waves, which determines the rank of the S matrix. This is not the case for the 100 orientation, when specular and Q reflection should be considered separately. This increases the rank of the S matrix and makes ultimate results for 100 junctions with finite transparencies strongly different compared to the 110 case. In the following, we focus solely on the 110 oriented interfaces.

For $d/\mathrm{AF}_{\mathrm{odd}}/d$ junctions, the general structure of the $\mathcal{S}$ matrix is similar to that of $d/\mathrm{F}/d$ junctions with symmetric F interfaces. This follows from the fact that in the (110) orientation and for an odd number of chains in the interlayer, all spins are aligned in the outermost chains. For (110) $d/\mathrm{AF}_{\mathrm{even}}/d$ junctions, the outermost chains of the AF interface have opposite spin polarizations (but still all aligned within each chain) and the $\mathcal{S}$ matrix is isomorphic to the three-layer ferromagnet-insulator-ferromagnet interface with antiparallel orientations of the two F layers.[15] The existence of the even-odd (0-π) behavior shown in Fig. 1(c) follows directly from this link between the $\mathcal{S}$ matrices for 110 $d/\mathrm{AF}/d$ and $d/\mathrm{F}/d$ junctions.[9] However, in order to understand the T dependence of $J_c(T)$ and obtain quantitative criteria for transitions between 0- and π-junction behaviors, we turn now to the explicit calculations.

Consider first the (110) $d/\mathrm{AF}_{\mathrm{even}}/d$ junctions where the transparency coefficients satisfy $D_\sigma = D_{\bar{\sigma}} = D = 1 - R$, resulting in the following Josephson current:

$$J(\chi,T) = \frac{e|\Delta^d|D\sin\chi}{\gamma}\tanh\left[\frac{|\Delta^d|\gamma}{2T}\right], \tag{3}$$

where $\gamma = \left(R\sin^2\frac{\Theta}{2} + D\cos^2\frac{\chi}{2}\right)^{1/2}$ and χ is the phase difference across the junction. Here, not only Δ^d and D, but also the spin-mixing parameter Θ $(\sin\Theta(k_y) = [m/2t\cos(k_y/\sqrt{2})]\{1+[m/4t\cos(k_y/\sqrt{2})]^2\}^{-1})$, are all k_y dependent, and the total current is a sum of Eq. (3) over all values of k_y.[9] However, as seen from Fig. 1(d), the k_y sum is unimportant for understanding the qualitative behavior. Equation (3) is valid for arbitrary transparency, and the critical current $J_c(T)$ is plotted in Fig. 2(a) for a range of Θ. In agreement with Fig. 1(a), the junction is always a 0 junction. Near T_c, Eq. (3) reduces to $J(\chi,T) = e|\Delta^d|^2 D\sin\chi/2T$ which coincides with the result in nonmagnetic (110) symmetric $d/I/d$ junctions. However, at low T, the current [Eq. (3)] is given by $J(\chi,T) = e|\Delta^d|D\sin\chi/\gamma$ which, in the tunneling limit, reduces to $J(\chi,T) = e|\Delta^d|D\sin\chi/|\sin\frac{\Theta}{2}|$. Therefore, due to the factor $|\sin\frac{\Theta}{2}|^{-1}$, we find the remarkable result that the current substantially exceeds the critical current in nonmagnetic (110) $d/I/d$ junctions with the same transparency coefficient D (Fig. 2).

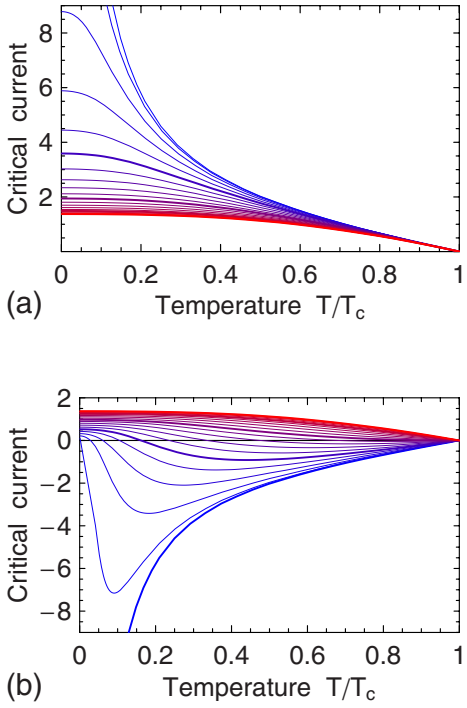

FIG. 2. (Color online) $J_c(T)$ obtained from quasiclassical calculations in the tunneling limit $D=0.001$ for $d/\mathrm{AF}_{\mathrm{even}}/d$ (a) and $d/\mathrm{AF}_{\mathrm{odd}}/d$ (b), plotted for different spin-mixing angles [from $\Theta=0$ (blue) to $\Theta=\pi$ (red) in intervals of 0.05π]. The k_y dependence of Θ has been neglected here.

Next, we discuss the T dependence of $J_c(T)$ for 110 $d/\mathrm{AF}_{\mathrm{odd}}/d$ junctions. As argued above, this junction is similar to 110 $d/\mathrm{F}/d$ junctions with symmetric F interlayer. In the tunneling limit, we obtain the following expression for $J_c(T)$ $(\alpha \equiv \pm 1)$,

$$J_c(T) = \alpha e|\Delta^d|\sqrt{D_\sigma D_{\bar{\sigma}}}\left[\sin\left(\frac{\Theta}{2}\right)\tanh\left(\frac{|\Delta^d|\sin\left(\frac{\Theta}{2}\right)}{2T}\right) - \frac{|\Delta^d|\cos^2\left(\frac{\Theta}{2}\right)}{2T}\cosh^{-2}\left(\frac{|\Delta^d|\sin\left(\frac{\Theta}{2}\right)}{2T}\right)\right], \tag{4}$$

which is plotted in Fig. 2(b) for $\alpha=1$ (see below). The result

for an arbitrary transparency can be obtained along similar lines to Ref. 16. In the absence of magnetism, when $\Theta=0$, $\alpha=-1$, and for zero transparency $D\to 0$, there are zero-energy Andreev bound states at both d/I surfaces of the (110) $d/I/d$ junction. With increasing Θ, the midgap states on each d/I surface evolve into spin-split Andreev states on a $d/\mathrm{F}I$ surface. For a given k_y, the energies of these spin-split states are $\varepsilon_d=\pm\Delta^d\sin(\frac{\Theta}{2})$. This is different from the s-wave case where $\varepsilon_s=\pm\Delta^s\cos(\frac{\Theta}{2})$,[17] and therefore, the behavior of the Josephson current in $s/\mathrm{F}/s$ tunnel junctions[16] strongly differs from d-wave magnetic junctions. Equation (4) can be qualitatively understood as follows: in tunnel junctions, the surface states ε_d further split and become phase dependent due to a finite transparency. As a result, four current-carrying interface Andreev states exist for a given k_y. Equation (4) represents the Josephson current carried by these states in the tunneling limit, when two spin-split surface states on each side of the junction only slightly overlap through the interlayer.

In the limit of a nonmagnetic interlayer ($\Theta=0$, $\alpha=-1$), only the second term in Eq. (4) survives and one obtains $J_c(T)=e|\Delta^d|^2D/2T$, with the well-known $1/T$ behavior for $d/I/d$ junctions. This result is the tunneling limit of the more general current-phase relation,[18,19]

$$J(\chi,T)=2e|\Delta^d|\sqrt{D}\sin\frac{\chi}{2}\tanh\left[\frac{|\Delta^d|}{2T}\sqrt{D}\cos\frac{\chi}{2}\right]. \qquad (5)$$

Hence, there are no 0-π transitions in (110) d-wave nonmagnetic junctions. This, however, is not the case in the presence of magnetic interlayers with finite spin-mixing Θ. Finite values of Θ result in the appearance of the additional (first) term in Eq. (4), which is comparatively small for small Θ, and has the opposite sign compared to the second term. The second term in Eq. (4) is, in its turn, strongly modified due to finite Θ at sufficiently low T. Indeed, it becomes exponentially small, if T is much less than the spin-split finite energies of the Andreev states ε_d. At the same time, for $\theta<\pi/2$ the second term in Eq. (4) dominates the current at higher T, for example, near T_c. For this reason, the 0-π transition arises in magnetic 110 $d/\mathrm{AF}_{\mathrm{odd}}/d$ tunnel junctions under the condition $\Theta<\pi/2$, as a result of the interplay of the two terms with opposite signs in Eq. (4). In principle, the change of sign of the total current in Eq. (4) takes place with varying T for any small value of Θ, but effects of finite transparency confine the conditions for the presence of a 0-π transition to not too small values of Θ.

For deriving the conditions for the presence of the 0-π transition in the tunneling limit, it is convenient to consider two limiting cases of Eq. (4): one near T_c and another at low T. Under the condition $\frac{|\Delta^d|}{2}\sin(\frac{\Theta}{2})\ll T\leqslant T_c$, Eq. (4) reduces to the simple expression,

$$J_c(T)=\frac{-\alpha e|\Delta^d|^2\sqrt{D_\sigma D_{\bar{\sigma}}}}{2T}\cos\Theta, \qquad (6)$$

which is suppressed by the factor $\cos\Theta$ compared to the corresponding nonmagnetic $d/I/d$ junction. Equation (6) is

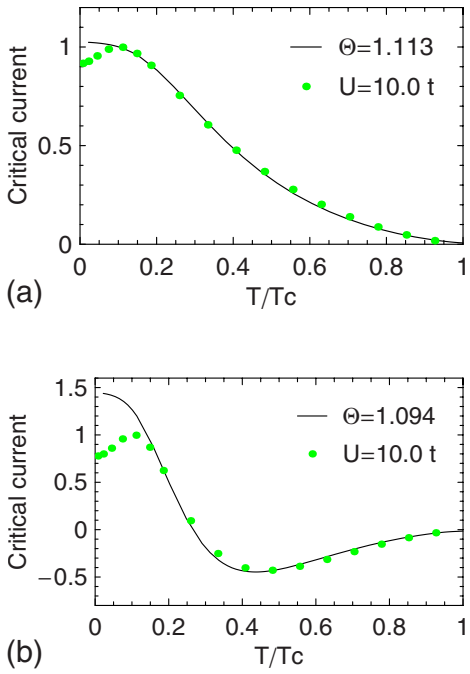

FIG. 3. (Color online) Critical current $J_c(T)$ versus temperature for (a) $d/\mathrm{AF}_{\mathrm{even}}/d$ and (b) $d/\mathrm{AF}_{\mathrm{odd}}/d$ junctions. The green dots display the same $U=10t$ BdG data points shown in Figs. 1(a) and 1(b) (normalized to 1.0). The solid curves are quasiclassical fits where the special choice $\cos k_y/\sqrt{2}=0.7$ has been taken, and the transparency D has been adjusted to fit the BdG data.

valid, in particular, near T_c. Under the opposite condition $T\ll\frac{|\Delta^d|}{2}\sin(\frac{\Theta}{2})$, Eq. (4) becomes

$$J_c(T)=\alpha e|\Delta^d|\sqrt{D_\sigma D_{\bar{\sigma}}}\left|\sin\left(\frac{\Theta}{2}\right)\right|, \qquad (7)$$

which is suppressed by the factor $|\sin(\frac{\Theta}{2})|$ compared to nonmagnetic $d/I/d$ junction. Comparing signs of Eqs. (6) and (7), it is evident that the 0-π transition takes place with varying T when $\cos\Theta>0$, that is, for $\Theta<\frac{\pi}{2}$. For $\alpha=1$ (which is the case for $d/\mathrm{AF}_{\mathrm{odd}}/d$ junctions) and $\Theta<\frac{\pi}{2}$, the 0 state is the ground state of the junction, whereas the π state exists near T_c in qualitative agreement with Fig. 1(b). Note that 0-π transitions in $s/\mathrm{F}/s$ junctions happen when the opposite inequality $\Theta>\frac{\pi}{2}$ is satisfied.[16] We stress that our results (4), (6), and (7) describe also the current in $d/\mathrm{F}/d$ junctions.

Above, we have extracted the form of the current characteristics in $d/\mathrm{AF}/d$ junctions via both numerical BdG methods and an analytical quasiclassical approach. An obvious question is how well these two methods agree. To this end, in Fig. 3, we plot again the BdG results (normalized to 1.0) for the case $U=10t$ with $L=6$ (left) and $L=5$ (right) and show self-consistent quasiclassical fits to these curves. Here, $\sin\Theta=m/2t\cos k_y/\sqrt{2}/[1+(m/4t\cos k_y/\sqrt{2})^2]$ and the special choice $\cos k_y/\sqrt{2}=0.7$ has been taken. The transparency D has been adjusted to fit the BdG data. As seen, there is overall very good agreement. At low T, some discrepancy can be detected, which we believe originates from the finite interlayer thickness used in the BdG calculations and/or the

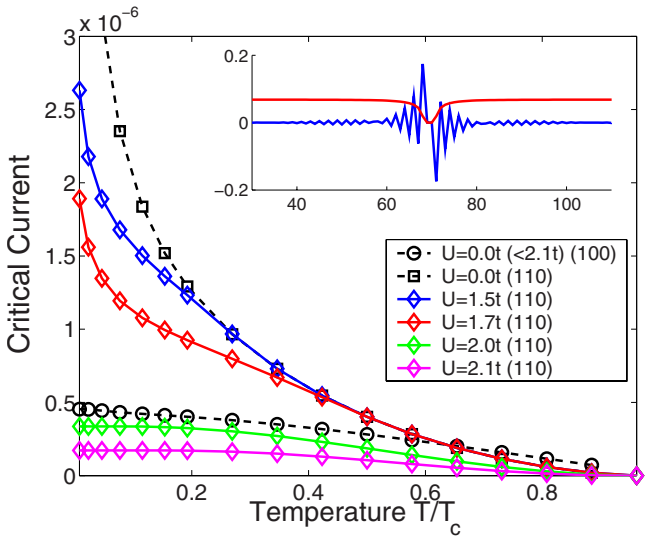

FIG. 4. (Color online) $J_c(T)$ versus T for 110 and 100 $d/I/d$ junctions with AF correlations in the d leads which have doping level $x=0.1$. The I region is modeled with $L=2$ and a potential of $V=30t$. In the 100 case, the same curve (black circles) is obtained for all $U\leqslant 2.1t$. (inset) Example of surface-induced magnetization (blue) and the suppression of Δ^d (red) at a 110 interface, shown here for $U=2.0t$.

different band structures (circular versus square Fermi surface in the quasiclassical and BdG approach, respectively). Disregarding any explicit k_y dependence of the transparency coefficients and the Θ parameter in the quasiclassical calculations may also play a role.

Experimental detection of 0-π transitions in $d/\mathrm{AF}/d$ junctions may be possible in sandwich structures of high-doped and undoped high-T_c materials similar to what was constructed for c-axis junctions.[20] Recently, Oh *et al.*[21] invented a spatially controlled doping method and fabricated in-plane 100 $d/\mathrm{AF}/d$ junctions. Our results show that the fabrication of similar 110 junctions and a detailed study of their Josephson current characteristics holds the promise of several unusual properties, as shown in Figs. 1 and 2. Realistic junctions will contain regions with varying interlayer thickness, but if these are sufficiently few, the regions with shortest thickness should dominate the current. Alternatively, one needs to average the current over interface imperfections. J_c in even junctions dominates at low T only in the limit of large U. Then, we have a small Θ and 0 junction with a low-T anomaly in J_c. Otherwise, critical currents in even and odd junctions are of the same order. For $\Theta>\pi/2$ (i.e., $m<4t$) the currents have identical signs at all T (0 junctions). For $\Theta<\pi/2$, the π-junction state arises in odd junctions near T_c, resulting in an overall cancellation of odd and even contributions to the current.

IV. GRAIN BOUNDARY JUNCTIONS

Finally, we turn to the question of J_c through grain boundaries, where a strong discrepancy between theory and experiment has been known for some time: when the GB is modeled as a $d/I/d$ junction, the zero-energy state existing in the 110 orientation results in a large low T increase of J_c as compared to the 100 orientation (see dashed lines in Fig. 4). However, the opposite behavior is obtained in experiments: J_c is the largest for 100 orientations and drops exponentially with increased angle between the GB and the crystal axis.[22] We model the GB using Eq. (1) in a $d/I/d$ geometry with a potential $V(n_{i\uparrow}+n_{i\downarrow})$ inside the insulating layer (I) and $U\neq 0$ in the leads only. For sufficiently small U, magnetization is absent in the superconducting leads, but the magnetic correlations can lead to instabilities near interfaces that suppress the d-wave superconductor order parameter,[23,24] as shown in the inset of Fig. 4. The main body of Fig. 4 shows $J_c(T)$ for a range of U all small enough not to induce magnetization in the bulk of the leads. Contrary to the 100 orientation, J_c through 110 GB can be significantly reduced by surface-induced magnetic order for $T<T_M$, where T_M is the critical temperature for the surface magnetization. In fact, as seen from Fig. 4, there exists a range of U where J_c at low T becomes smaller in the 110 orientation compared to the 100. This shows the importance of competing surface effects even though a complete understanding of the physics of GB junctions requires more detailed microscopic calculations.

V. CONCLUSIONS

We have studied the dc Josephson current through $d/\mathrm{AF}/d$ tunnel junctions as a function of interlayer thickness and temperature using both numerical BdG diagonalization and analytical quasiclassical methods. For an odd (even) number of antiferromagnetic chains in the interlayer, the current characteristics of 110 oriented interfaces display π (0)-junction behavior. In addition, $d/\mathrm{AF}_{\mathrm{odd}}/d$ junctions can exhibit π-0 transitions as a function of temperature. We have shown that in terms of the spin-mixing parameter Θ, the condition for the latter is given by $\Theta<\frac{\pi}{2}$. This is the opposite regime as compared to leads with s-wave pairing symmetry where temperature-induced π-0 transitions take place for $\Theta>\frac{\pi}{2}$. Another important difference between $s/\mathrm{AF}/s$ and $d/\mathrm{AF}/d$ junctions exists for the 100 orientation, where d-wave junctions are always 0 junctions whereas this is not the case for s-wave superconductors. Finally, we studied grain boundary junctions modeled as $d/I/d$ junctions but with subdominant magnetic correlations in the superconducting leads. This allows for interface-induced magnetism near grains which tend to suppress the d-wave order parameter. We showed that this mechanism can lead to larger critical currents for the 100 orientation than for 110, in qualitative agreement with experiments.

ACKNOWLEDGMENTS

B.M.A. acknowledges support from the Villum Kann Rasmussen Foundation. Partial support for this research was provided by DOE under Grant No. DE-FG02-05ER46236. Yu.S.B. acknowledges the support of RFBR grant (05-02-17175). Numerical calculations were performed at the University of Florida High-Performance Computing Center (http://hpc.ufl.edu).

[1] A. I. Buzdin, Rev. Mod. Phys. **77**, 935 (2005).
[2] V. V. Ryazanov, V. A. Oboznov, A. Yu. Rusanov, A. V. Veretennikov, A. A. Golubov, and J. Aarts, Phys. Rev. Lett. **86**, 2427 (2001).
[3] T. Kontos, M. Aprili, J. Lesueur, F. Genêt, B. Stephanidis, and R. Boursier, Phys. Rev. Lett. **89**, 137007 (2002).
[4] L. N. Bulaevskii, V. V. Kuzii, and A. A. Sobyanin, JETP Lett. **25**, 290 (1977).
[5] E. Terzioglu and M. R. Beasley, IEEE Trans. Appl. Supercond. **8**, 48 (1998).
[6] I. Zutić, J. Fabian, and S. Das Sarma, Rev. Mod. Phys. **76**, 323 (2004).
[7] I. V. Bobkova, P. J. Hirschfeld, and Yu. S. Barash, Phys. Rev. Lett. **94**, 037005 (2005).
[8] B. M. Andersen, I. V. Bobkova, P. J. Hirschfeld, and Yu. S. Barash, Phys. Rev. B **72**, 184510 (2005).
[9] B. M. Andersen, I. V. Bobkova, P. J. Hirschfeld, and Yu. S. Barash, Phys. Rev. Lett. **96**, 117005 (2006).
[10] Yu. S. Barash, H. Burkhardt, and D. Rainer, Phys. Rev. Lett. **77**, 4070 (1996).
[11] Y. Tanaka and S. Kashiwaya, Phys. Rev. B **53**, R11957 (1996).
[12] E. Il'ichev, M. Grajcar, R. Hlubina, R. P. J. IJsselsteijn, H. E. Hoenig, H.-G. Meyer, A. Golubov, M. H. S. Amin, A. M. Zagoskin, A. N. Omelyanchouk, and M. Y. Kupriyanov, Phys. Rev. Lett. **86**, 5369 (2001).
[13] G. Testa, A. Monaco, E. Esposito, E. Sarnelli, D.-J. Kang, S. H. Mennema, E. J. Tarte, and M. G. Blamire, Appl. Phys. Lett. **85**, 1202 (2004).
[14] G. Testa, E. Sarnelli, A. Monaco, E. Esposito, M. Ejrnaes, D.-J. Kang, S. H. Mennema, E. J. Tarte, and M. G. Blamire, Phys. Rev. B **71**, 134520 (2005).
[15] Yu. S. Barash, I. V. Bobkova, and T. Kopp, Phys. Rev. B **66**, 140503(R) (2002).
[16] Yu. S. Barash and I. V. Bobkova, Phys. Rev. B **65**, 144502 (2002).
[17] M. Fogelström, Phys. Rev. B **62**, 11812 (2000).
[18] R. A. Riedel and P. F. Bagwell, Phys. Rev. B **57**, 6084 (1998).
[19] Y. Tanaka and S. Kashiwaya, Rep. Prog. Phys. **63**, 1641 (2000).
[20] I. Bozovic, G. Logvenov, M. A. J. Verhoeven, P. Caputo, E. Goldobin, and T. H. Geballe, Nature (London) **422**, 873 (2003).
[21] S. Oh, J. A. Bonetti, K. Inderhees, D. J. Van Harlingen, and J. N. Eckstein, Appl. Phys. Lett. **87**, 231911 (2005).
[22] H. Hilgenkamp and J. Mannhart, Rev. Mod. Phys. **74**, 485 (2002).
[23] Y. Ohashi, Phys. Rev. B **60**, 15388 (1999).
[24] C. Honerkamp, K. Wakabayashi, and M. Sigrist, Europhys. Lett. **50**, 368 (2000).